SIAM J. APPL. MATH.
Vol. 73, No. 2, pp. 741–756

A MULTISCALE METHOD FOR OPTICAL RESPONSES OF NANOSTRUCTURES*

GANG BAO†, DI LIU‡, AND SONGTING LUO§

Abstract. We introduce a new framework for the multiphysical modeling and multiscale computation of nano-optical responses. The semiclassical theory treats the evolution of the electromagnetic field and the motion of the charged particles self-consistently by coupling Maxwell equations with quantum mechanics. To overcome the numerical challenge of solving the high-dimensional many-body Schrödinger equations involved, we adopt the time-dependent current density functional theory. In the regime of linear responses, this leads to a linear system of equations determining the electromagnetic field as well as the current and electron densities simultaneously. A self-consistent multiscale method is proposed to deal with the well-separated space scales. Numerical examples are presented to illustrate the resonant condition.

Key words. optical response, nanostructures, multiscale methods

AMS subject classifications. 78A45, 81-08, 81V55

DOI. 10.1137/12087147X

1. Introduction.

The study of optical responses of nanostructures has raised a lot of interest in the development of modern physics with many important applications such as near field optical microscopy, resonant photonic crystals, optical computing, and molecular sensing. From the modeling point of view, when the optical device is of nanoscale, the macroscopic theory for the electromagnetic (EM) field cannot faithfully capture the microscopic and nonlocal character of the light-matter interaction. In this case, it is necessary to consider the quantum mechanical description of the current and charge densities. On the theoretical side, quantum electrodynamics (QED) [7] is able to give a complete description of the interactions between photons and electrons. However, the high computational expense prohibits QED from applications to complex systems. To avoid the high complexity of QED, the semiclassical theories [21, 16, 6] combine the classical treatment of the EM field and the first principle approach for the charged particles. Different from QED, in a semiclassical theory, the EM field is not quantized and its evolution is described classically by the Maxwell equations. In the meantime, the motion of the charged particles is determined quantum mechanically by the Schrödinger equations. Similarly to QED, the EM field as well as the current and charge densities must be determined self-consistently through the coupled system of Maxwell and Schrödinger equations.

Although the semiclassical approach reduces the high computational cost of QED, a many-body Schrödinger equation is still involved. For many practical problems,

*Received by the editors March 27, 2012; accepted for publication (in revised form) December 27, 2012; published electronically March 26, 2013. This research was supported in part by NSF Focused Research Group grant DMS-0968360.

http://www.siam.org/journals/siap/73-2/87147.html

†Department of Mathematics, Zhejiang University, Hangzhou 310027, China; and Department of Mathematics, Michigan State University, East Lansing, MI 48824 (bao@math.msu.edu). The research of this author was supported in part by NSF grants DMS-0908325, DMS-0968360, DMS-1211292, ONR grant N00014-12-1-0319, a Key Project of the Major Research Plan of NSFC (91130004), and a special research grant from Zhejiang University.

‡Department of Mathematics, Michigan State University, East Lansing, MI 48824 (richardl@math.msu.edu).

§Department of Mathematics, Iowa State University, Ames, IA 50011 (luos@iastate.edu).

solving a high-dimensional many-body Schrödinger equation is prohibitively expensive. In this paper, we adopt the time-dependent current density functional theory (TD-CDFT) [20, 13] to further simplify the model and its computation. In the density functional theory (DFT) for the ground state of the charged particles, a one-to-one correspondence (up to an arbitrary constant) between the external potential and the ground state electron density has been proved in the seminal work of Hohenberg and Kohn [14]. Hence, the wavefunction can be obtained as a functional of the electron density, which allows the evaluation of all observables of the system. Similar results have been extended to the case of time evolutionary electronic structures in the form of time-dependent density functional theory (TD-DFT) by Runge and Gross [20], and later to the situation of external electric and magnetic fields with arbitrary time dependence by Ghosh and Dhara [13] in the form of TD-CDFT, where the current density is introduced as the fundamental variable. Based on the one-to-one correspondence between the electron (or current) density, the external potential, and the wavefunction, a synthetic noninteracting many-body system under an effective external potential is introduced to produce in principle the same current and electron densities as those of the original interacting many-body system. Therefore a practical scheme called the Kohn–Sham (KS) system [17] can be designed to calculate the current and electron densities, which greatly simplifies the computation. In the KS system, the many-body effects are included via the so-called exchange-correlation (xc) potentials.

The purpose of the present paper is to incorporate TD-CDFT into the framework of the semiclassical optical response theory, thereby avoiding the computational cost of solving the many-body Schrödinger equation. We call the so-obtained system the density functional semiclassical theory for nano-optics, which is formulated as coupled Maxwell–Kohn–Sham (Maxwell-KS) equations (also see [3, 18, 9] for similar models). In the regime of linear responses, a system of linear equations for self-consistently determining the EM field, the current density, and the electron density can be derived. Moreover, the zero eigenvalue problem of the linear system corresponds to the resonant eigenmodes [6] of the nano-optical response. To deal with the disparate space scales of the system, we propose a multiscale scheme which can solve the system self-consistently by allowing communications between the macrosolver for the Maxwell equations and the microsolver for the KS equations.

The rest of the paper is organized as follows. In section 2, we incorporate TD-CDFT into the semiclassical theory and form the Maxwell-KS equations. Then in section 3 we provide the linear response theory for the density functional semiclassical theory. A multiscale solver to solve the linear system is introduced in section 4, following the demonstration of the multiscale nature of the problem through a simple example. Finally, in section 5, numerical examples are presented to illustrate the validity of the method. Throughout the paper, atomic units ($e = \hbar = m = 1$) are used. We will also represent vector variables in boldface and scalar variables in the normal font.

2. Density functional semiclassical theory of nano-optics. We first introduce a framework for the modeling and computation of nano-optical responses by combining the semiclassical theory and TD-CDFT. Mathematically, the system is described by the coupled Maxwell–Kohn–Sham (Maxwell-KS) equations.

2.1. Semiclassical theory. The semiclassical theory for nano-optical responses adopts classical treatments of the EM field and quantum mechanical descriptions of the charged particles. To present the theory briefly, we follow the notation in [6]. The evolution of the EM field can be determined by the Maxwell equations. In terms of

the vector potential $\mathbf{A}$ and the scalar potential ϕ, under the Coulomb gauge $\nabla\cdot\mathbf{A}=0$, the Maxwell equations have the form

$$\begin{aligned}\frac{1}{c^2}\frac{\partial^2\mathbf{A}}{\partial t^2}-\nabla^2\mathbf{A}+\frac{1}{c}\frac{\partial(\nabla\phi)}{\partial t}&=\frac{4\pi}{c}\mathbf{j},\\ -\nabla^2\phi&=4\pi\rho,\end{aligned}\tag{2.1}$$

where c is the speed of light in vacuum, and $\mathbf{j}$ and ρ are the current and charge densities related by the continuity equation:

$$\nabla\cdot\mathbf{j}+\frac{\partial\rho}{\partial t}=0.\tag{2.2}$$

The electric and magnetic fields, $\mathbf{E}$ and $\mathbf{B}$, can be evaluated by

$$\mathbf{E}=-\nabla\phi-\frac{1}{c}\frac{\partial\mathbf{A}}{\partial t}\quad\text{and}\quad\mathbf{B}=\nabla\times\mathbf{A}.\tag{2.3}$$

Notice that in the Maxwell equations, ρ and $\mathbf{j}$ serve as inputs to compute the EM field. In a classical macroscopic model, they would be determined by the so-called constitutive relations as local functions in terms of $\mathbf{E}$ and $\mathbf{B}$. When the size of the sample is of nanoscale such that the spatial structure of the resonant states is comparable to or even larger than the wavelength of the light, a microscopic nonlocal treatment must be considered.

Quantum mechanically, the motion of the charged particles is governed by the Schrödinger equation. For simplicity, we will assume the Born–Oppenheimer approximation to separate the electronic motion and the nuclear motion for the molecular structures under consideration. For a system consisting of N electrons moving under the influence of a given transverse EM field represented by $\mathbf{A}$, the general nonrelativistic Hamiltonian takes the form [6, 7]

$$H_M=\frac{1}{2}\sum_l\left[\mathbf{p}_l+\frac{1}{c}\mathbf{A}(\mathbf{r}_l)\right]^2+\sum_l v(\mathbf{r}_l)+U,\tag{2.4}$$

where $\mathbf{r}_l$ and $\mathbf{p}_l$ are the coordinate and conjugate momentum of the lth electron, $v(\mathbf{r})$ is the single particle external potential due to the nuclei, and $U=\frac{1}{2}\sum_{l\neq l'}1/|\mathbf{r}_l-\mathbf{r}_{l'}|$ is the mutual Coulomb interaction among electrons. The Hamiltonian H_M can be decomposed as

$$H_M=H_0+H_{int},\tag{2.5}$$

such that

$$\begin{aligned}H_0&=\frac{1}{2}\sum_l{\mathbf{p}_l}^2+\sum_l v(\mathbf{r}_l)+U,\\ H_{int}&=\sum_l\left(\frac{1}{c}\mathbf{A}_l\cdot\mathbf{p}_l+\frac{1}{2c^2}\mathbf{A}_l^2\right),\end{aligned}\tag{2.6}$$

where H_0 and H_{int} can be regarded as the matter Hamiltonian and the radiation-matter interaction, respectively. For the physical situation under consideration, we assume that at time t_0, the matter system is at the ground state ψ_0 with energy E_0 satisfying the eigenvalue problem

$$H_0\psi_0(\mathbf{r}_1,\ldots,\mathbf{r}_N)=E_0\psi_0(\mathbf{r}_1,\ldots,\mathbf{r}_N).\tag{2.7}$$

After the incident light is applied, the system will evolve according to the time-dependent Schrödinger equation

$$i\frac{\partial\psi(\mathbf{r}_1,\ldots,\mathbf{r}_N,t)}{\partial t} = H_M\psi(\mathbf{r}_1,\ldots,\mathbf{r}_N,t). \tag{2.8}$$

The current density $\mathbf{j}(\mathbf{r},t)$ and the electron density $\rho(\mathbf{r},t)$ can be computed, respectively, through the solution of (2.8) using

$$\mathbf{j}(\mathbf{r},t) = \langle\psi|\hat{\mathbf{j}}|\psi\rangle \quad \text{and} \quad \rho(\mathbf{r},t) = \langle\psi|\hat{\rho}|\psi\rangle\,, \tag{2.9}$$

with the current density operator $\hat{\mathbf{j}}$ and the electron density operator $\hat{\rho}$ given, respectively, by

$$\begin{aligned}\hat{\mathbf{j}} &= -\frac{1}{2}\sum_l\Big[\mathbf{p}_l\delta(\mathbf{r}-\mathbf{r}_l)+\delta(\mathbf{r}-\mathbf{r}_l)\mathbf{p}_l\Big]-\frac{1}{c}\sum_l\mathbf{A}(\mathbf{r}_l,t) \quad \text{and}\\ \hat{\rho} &= -\sum_l\delta(\mathbf{r}-\mathbf{r}_l).\end{aligned} \tag{2.10}$$

Notice that in the Schrödinger equation (2.8), $\mathbf{A}$ acts as the parameter for computing the wavefunction ψ, which will facilitate the computation of all physical observables including the current and electron densities.

In the semiclassical model, the system is completely described by $(\mathbf{A},\phi)$ and ψ, which affect each other through the coupled Maxwell equations (2.1) and Schrödinger equation (2.8). Therefore they must be determined self-consistently so that (2.1) and (2.8) are solved concurrently, which will give rise to the evolution of the EM field and the motion of the electrons simultaneously.

2.2. Time-dependent current density functional theory. Although the semiclassical theory greatly simplifies the modeling of light-matter interactions at nanoscales, it still poses a significant numerical challenge to solve the many-body Schrödinger equation involved. The wavefunction $\psi(\mathbf{r}_1,\ldots,\mathbf{r}_N,t)$ is a function of $3N$-dimensional ($3N$-D) spatial variables, which means it is in general too complicated to solve the Schrödinger equation either analytically or numerically for many applications in nano-optics, except for cases with special symmetries. On the other hand, notice that solving the Maxwell equations (2.1) only requires much simpler input quantities, i.e., the current density $\mathbf{j}$ and the electron density ρ. One efficient way to obtain numerical approximations of $(\mathbf{j},\rho)$ is the time-dependent current density functional theory (TD-CDFT). The advantage of TD-CDFT is that by restricting calculations to the current and electron densities that are functions of only 3-D spatial variables, the computational cost can be greatly reduced.

The density functional theory (DFT) was originally designed to calculate the ground state electron density. For the ground state wavefunction ψ_0 satisfying (2.7), the well-known Hohenberg–Kohn theorem [14] indicates that the electron density ρ can be considered as the basic variable to describe a quantum mechanical system such that each observable of the system is a functional in terms of ρ. Following the Hohenberg–Kohn theorem, Kohn and Sham [17] provided a practical scheme to calculate ρ based on a hypothetical system of noninteracting electrons that is supposed to have the same electron density as that of the physical system under consideration. A system of Kohn–Sham (KS) equations can be derived as

$$H_0^{KS}\psi_l(\mathbf{r}) = \epsilon_l\psi_l(\mathbf{r}), \tag{2.11}$$

where

$$H_0^{KS} = \frac{1}{2}\mathbf{p}^2 + v_{KS}(\mathbf{r}). \tag{2.12}$$

The effective KS potential $v_{KS}(\mathbf{r})$ is given by

$$v_{KS}(\mathbf{r}) = v(\mathbf{r}) + v_H(\mathbf{r}) + v_{xc}(\mathbf{r}), \tag{2.13}$$

where $v(\mathbf{r})$ is the external potential and $v_H(\mathbf{r})$ is the Hartree potential:

$$v_H(\mathbf{r}) = \int d\mathbf{r}' \frac{\rho(\mathbf{r}')}{|\mathbf{r} - \mathbf{r}'|}. \tag{2.14}$$

The term $v_{xc}(\mathbf{r}) \equiv \delta E_{xc}[\rho]/\delta\rho$ represents the exchange-correlation (xc) potential containing the many-body effects with $E_{xc}[\rho]$ being the xc energy functional. The electron density is then given by

$$\rho(\mathbf{r}) = \sum_l f_l |\psi_l(\mathbf{r})|^2, \tag{2.15}$$

where f_l is the occupation number corresponding to orbital ψ_l. Notice that the KS equation involves the unknown $\psi_l(\mathbf{r})$ that depends only on 3-D spatial variables, which greatly reduces the computational cost.

The DFT has been extended as the time-dependent density functional theory (TD-DFT) by Runge–Gross [20] for time-dependent systems and as time-dependent current density functional theory (TD-CDFT) by Ghosh and Dhara [13] for time-dependent systems under the influence of both electric and magnetic fields. For a system satisfying the Schrödinger equation (2.8) that is able to describe electron excitations under external influences, a system of time-dependent KS equations can also be derived in TD-CDFT [13] in the form

$$i\frac{\partial\psi_l(t)}{\partial t} = H_M^{KS}(t)\psi_l(t), \tag{2.16}$$

with the Hamiltonian

$$H_M^{KS}(t) = \frac{1}{2}\Big[\mathbf{p} + \mathbf{A}_{KS}(\mathbf{r},t)\Big]^2 + v_{KS}(\mathbf{r},t). \tag{2.17}$$

The time-dependent KS potential in the above Hamiltonian is given by

$$v_{KS}(\mathbf{r},t) = v(\mathbf{r},t) + v_H(\mathbf{r},t) + v_{xc}(\mathbf{r},t), \tag{2.18}$$

with $v_{xc}(\mathbf{r},t)$ representing the time-dependent scalar xc-potential, and

$$\mathbf{A}_{KS}(\mathbf{r},t) = \frac{1}{c}\mathbf{A}(\mathbf{r},t) + \frac{1}{c}\mathbf{A}_{xc}(\mathbf{r},t), \tag{2.19}$$

where $\mathbf{A}$ is the vector potential for the external transverse EM field and $\mathbf{A}_{xc}(\mathbf{r},t)$ is the vector xc-potential. In addition to the electron density given by (2.15), we can also obtain the current density by

$$\begin{aligned}\mathbf{j}(\mathbf{r},t) = -\frac{i}{2}\sum_l f_l\Big[\psi_l^*(\mathbf{r},t)\nabla\psi_l(\mathbf{r},t) - \psi_l(\mathbf{r},t)\nabla\psi_l^*(\mathbf{r},t)\Big] \\ + \sum_l f_l|\psi_l(\mathbf{r})|^2\mathbf{A}_{KS}(\mathbf{r},t),\end{aligned} \tag{2.20}$$

with f_l being the occupation number corresponding to orbital ψ_l. Notice that TD-CDFT provides a much simpler way to evaluate the electron density ρ and the current density $\mathbf{j}$ by reducing the dimension of the problem. Instead of solving the many-body Schrödinger equation (2.8) with $3N$-D spatial variables, we can solve the 3-D KS equations (2.16) to obtain ρ and $\mathbf{j}$. It should be pointed out that while the basic variable in DFT and TD-DFT is the electron density ρ, in TD-CDFT the basic variable turns out to be the current density $\mathbf{j}$, in the sense that once $\mathbf{j}$ is obtained, ρ can also be solved through the continuity equation (2.2).

In practice, both the scalar xc-potential v_{xc} and the vector xc-potential $\mathbf{A}_{xc}$ need to be approximated. For applications in this paper, the local density approximation (LDA) and the adiabatic local density approximation (ALDA) are used for v_{xc} in the ground state case and the time-dependent case, respectively [10, 19]. For the vector xc-potential $\mathbf{A}_{xc}$, the Vignale–Kohn (VK) functional [24, 25] is used. In LDA, the exchange-correlation energy functional is given by

$$E_{xc}[\rho] = \int \rho(\mathbf{r})\epsilon_{xc}\big(\rho(\mathbf{r})\big)d\mathbf{r}, \tag{2.21}$$

where $\epsilon_{xc}(\rho)$ is the exchange-correlation energy per particle for a homogeneous electron gas evaluated at the local density $\rho(\mathbf{r})$. The functional $\epsilon_{xc}(\rho)$ can be further split into an exchange part $\epsilon_x(\rho)$ and a correlation part $\epsilon_c(\rho)$ such that $\epsilon_x(\rho)$ is given by the Dirac exchange-energy functional [8]:

$$\epsilon_x(\rho) = -\frac{3}{4}\left(\frac{3\rho}{\pi}\right)^{1/3}. \tag{2.22}$$

For $\epsilon_c(\rho)$, the parametrization of Vosko, Wilk, and Nusair [26] is adopted. Then v_{xc} is given as the functional derivative of $E_{xc}[\rho]$:

$$v_{xc}(\mathbf{r}) = \frac{\delta E_{xc}[\rho]}{\delta\rho}. \tag{2.23}$$

ALDA is a straightforward extension of LDA where the static LDA functional is used for the dynamical properties but evaluated at the time-dependent electron density, i.e.,

$$v_{xc}(\mathbf{r},t) = v_{xc}\big(\rho(\mathbf{r},t)\big). \tag{2.24}$$

The VK functional is derived on the basis of the properties of the inhomogeneous electron gas [24] with the following form in the frequency domain [25]: the kth-component of $\mathbf{A}_{xc}$ is given as

$$\mathbf{A}_{xc,k}(\mathbf{r},\omega) = \frac{1}{(i\omega)}\left(\partial_k v_{xc} - \frac{1}{\rho_0(\mathbf{r})}\sum_j \partial_j \sigma_{xc,kj}(\mathbf{r},\omega)\right), \quad k = 1,2,3, \tag{2.25}$$

where ρ_0 is the ground state electron density and σ_{xc} is a viscoelastic stress tensor [25, 23].

2.3. The Maxwell-KS equations. We can incorporate TD-CDFT into the semiclassical theory by replacing the current and electron densities (2.9) given by the solution of the Schrödinger equation with those obtained by TD-CDFT using (2.15) and (2.20). Therefore the Maxwell equations (2.1) and the time-dependent KS

equations (2.16) form a coupled system for the EM field ($\mathbf{A}$, ϕ) and the current and electron densities ($\mathbf{j}$, ρ) as they are functionals of each other, i.e.,

$$\begin{cases} (\mathbf{A}, \phi) = \mathcal{M}[\mathbf{j}, \rho]; \\ (\mathbf{j}, \rho) = \mathcal{T}[\mathbf{A}, \phi], \end{cases} \tag{2.26}$$

which suggests that they must be determined self-consistently. From now on, we will refer to the above equations as the Maxwell–Kohn–Sham (Maxwell-KS) equations for nano-optics. Systems coupling the Maxwell equations and TD-DFT without using the current density have also been proposed in [3, 9]. Different from the TD-CDFT-based Maxwell-KS model proposed in [18], we have followed the approach in [6] to adopt the Coulomb gauge; therefore the EM field $\mathbf{A}$ consists of only the transverse component. The model is multiphysical in nature. As explained in later sections, it also poses a multiscale challenge for numerical solutions.

3. Linear response of the semiclassical theory. By computing the current and electron densities with TD-CDFT in the semiclassical theory for nano-optical responses, we are able to greatly simplify the system by reducing its dimension. In this section, we formulate the linear response of the Maxwell-KS system (2.26), which will further facilitate the computation. In the regime of linear responses, the self-consistent calculation of $(\mathbf{A}, \phi)$ and $(\mathbf{j}, \rho)$ results in a simple linear system of equations that will allow us to work in the frequency domain.

3.1. Linearized Maxwell-KS equations. As mentioned above, the physical context is the optical response of a matter system, initially in the ground state, to an EM field switched on externally. Rewriting the Maxwell equations in the integral form through Green functions shows that the EM field is actually linear functionals of the current and electron densities. On the other hand, the linear response theory of TD-CDFT [23, 24, 4] describes the linear relation between the input EM field and the output microscopic quantities. Combining both theories will lead to the following linear system for the induced EM field ($\delta\mathbf{A}$, $\delta\phi$) and the induced current and electron densities ($\delta\mathbf{j}$, $\delta\rho$):

$$\begin{cases} \delta\mathbf{A}(\mathbf{r}, \omega) = -\dfrac{1}{c} \displaystyle\int \mathbf{G}(\mathbf{r} - \mathbf{r}')\delta\mathbf{j}(\mathbf{r}')d\mathbf{r}', \\ \delta\phi(\mathbf{r}, \omega) = -\displaystyle\int \frac{\delta\rho(\mathbf{r}')}{|\mathbf{r} - \mathbf{r}'|}d\mathbf{r}', \\ \delta\mathbf{j}(\mathbf{r}, \omega) = \displaystyle\int \Big(\chi_{jj}(\mathbf{r}, \mathbf{r}', \omega) - \chi_{jj}(\mathbf{r}, \mathbf{r}', 0)\Big) \cdot \delta\mathbf{A}_{KS}(\mathbf{r}', \omega)d\mathbf{r}' \\ \qquad\qquad + \displaystyle\int \chi_{j\rho}(\mathbf{r}, \mathbf{r}', \omega)\delta v_{KS}(\mathbf{r}', \omega)d\mathbf{r}', \\ \delta\rho(\mathbf{r}, \omega) = \displaystyle\int \chi_{\rho j}(\mathbf{r}, \mathbf{r}', \omega) \cdot \delta\mathbf{A}_{KS}(\mathbf{r}', \omega)d\mathbf{r}' \\ \qquad\qquad + \displaystyle\int \chi_{\rho\rho}(\mathbf{r}, \mathbf{r}', \omega)\delta v_{KS}(\mathbf{r}', \omega)d\mathbf{r}', \end{cases} \tag{3.1}$$

where the vector and scalar potentials, $\delta\mathbf{A}_{KS}$ and δv_{KS}, are linear functionals in terms of $\delta\mathbf{A}$, $\delta\mathbf{j}$, and $\delta\rho$ such that

$$\delta\mathbf{A}_{KS}(\mathbf{r}, \omega) = \frac{1}{c}(\mathbf{A}_0(\mathbf{r}, \omega) + \delta\mathbf{A}(\mathbf{r}, \omega)) + \int \mathbf{f}_{xc}(\mathbf{r}, \mathbf{r}', \omega)\delta\mathbf{j}(\mathbf{r}', \omega)d\mathbf{r}', \tag{3.2}$$

and

$$\delta v_{KS}(\mathbf{r},\omega) = \int \frac{\delta\rho(\mathbf{r}',\omega)}{|\mathbf{r}-\mathbf{r}'|}d\mathbf{r}' + \int f_{xc}(\mathbf{r},\mathbf{r}',\omega)\delta\rho(\mathbf{r}',\omega)d\mathbf{r}', \tag{3.3}$$

with $\mathbf{f}_{xc} \equiv 1/c(\delta\mathbf{A}_{xc}/\delta\mathbf{j})$ and $f_{xc} \equiv \delta v_{xc}/\delta\rho$ being the tensor and scalar xc-kernels, respectively. $\mathbf{A}_0$ is the incident light. The tensorial Green function $\mathbf{G}$ can be given as

$$\mathbf{G}(\mathbf{r}-\mathbf{r}') = \frac{e^{iq|\mathbf{r}-\mathbf{r}'|}}{|\mathbf{r}-\mathbf{r}'|}\mathbf{I} + \frac{1}{q^2}\left(\frac{e^{iq|\mathbf{r}-\mathbf{r}'|}}{|\mathbf{r}-\mathbf{r}'|} - \frac{1}{|\mathbf{r}-\mathbf{r}'|}\right)\nabla'\nabla', \tag{3.4}$$

where $q = \omega/c$ is the wavenumber in a vacuum. The linear response function is given by

$$\begin{aligned}&\chi_{\alpha\beta}(\mathbf{r},\mathbf{r}',\omega)\\ &= \sum_{ia} f_i\left[\left(\frac{\psi_i(\mathbf{r})\alpha\psi_a(\mathbf{r})\psi_a(\mathbf{r}')\beta\psi_i(\mathbf{r}')}{\epsilon_i-\epsilon_a+\omega}\right) - \left(\frac{\psi_i(\mathbf{r})\alpha\psi_a(\mathbf{r})\psi_a(\mathbf{r}')\beta\psi_i(\mathbf{r}')}{\epsilon_a-\epsilon_i+\omega}\right)^*\right],\end{aligned} \tag{3.5}$$

where i and a run over the occupied and unoccupied KS orbitals of (2.11), respectively. The electron density operator $\boldsymbol{\rho} = 1$ and the following paramagnetic current density operator should be substituted for α and β in (3.5):

$$\mathbf{j}_p = -i(\nabla - \nabla^\dagger)/2, \tag{3.6}$$

with $\nabla^\dagger$ acting on the term to the left. Notice that $(\delta\mathbf{j},\ \delta\rho)$ in the above equations satisfy the continuity equation in the frequency domain such that

$$\delta\rho = \frac{1}{i\omega}\nabla\cdot\delta\mathbf{j}\ . \tag{3.7}$$

3.2. *P*-matrix formulation. To further simply the notation, we choose the following spectral representations for the current and electron densities:

$$\begin{aligned}\delta\mathbf{j}(\mathbf{r},\omega) &= \sum_{ia} f_i\frac{-\omega}{\epsilon_i-\epsilon_a}\psi_i(\mathbf{r})\mathbf{j}_p\psi_a(\mathbf{r})\big[P_{ai}(\omega) - P_{ia}(\omega)\big],\\ \delta\rho(\mathbf{r},\omega) &= \sum_{ia} f_i\psi_i(\mathbf{r})\psi_a(\mathbf{r})\big[P_{ai}(\omega) - P_{ia}(\omega)\big],\end{aligned} \tag{3.8}$$

with the P-matrix elements defined to be

$$\begin{aligned}&P_{ml}(\omega)\\ &= \frac{\dfrac{-\omega}{\epsilon_l-\epsilon_m}\displaystyle\int \psi_m(\mathbf{r})\mathbf{j}_p\psi_l(\mathbf{r})\cdot\delta\mathbf{A}_{KS}(\mathbf{r},\omega)d\mathbf{r} + \int \psi_m(\mathbf{r})\psi_l(\mathbf{r})\delta v_{KS}(\mathbf{r},\omega)d\mathbf{r}}{\epsilon_l-\epsilon_m+\omega}\end{aligned} \tag{3.9}$$

for $\{m,l\} = \{i,a\}$ or $\{a,i\}$. It is shown in Appendix A that the above formulation is consistent with the last two equations in the linear Maxwell-KS equations (3.1). Substituting (3.8) into the first two equations in (3.1) leads to

$$\begin{aligned}\delta\mathbf{A}(\mathbf{r},\omega) &= \sum_{ia} f_i\frac{\omega}{c(\epsilon_i-\epsilon_a)}\\ &\qquad\times\int \mathbf{G}(\mathbf{r}-\mathbf{r}')\psi_i(\mathbf{r}')\mathbf{j}_p\psi_a(\mathbf{r}')d\mathbf{r}'\big[P_{ai}(\omega) - P_{ia}(\omega)\big],\\ \delta\phi(\mathbf{r},\omega) &= \sum_{ia} f_i\int\frac{\psi_i(\mathbf{r}')\psi_a(\mathbf{r}')}{|\mathbf{r}-\mathbf{r}'|}d\mathbf{r}'\big[P_{ai}(\omega) - P_{ia}(\omega)\big].\end{aligned} \tag{3.10}$$

By eliminating $(\delta\mathbf{A}_{KS},\ \delta v_{KS})$ and $(\delta\mathbf{j},\ \delta\rho)$ in (3.2)–(3.3), (3.8), and (3.9), we arrive at a linear system satisfied by the elements of the P-matrix such that for j and b running over occupied and unoccupied orbitals respectively, we have

$$\begin{aligned} P_{jb}(\omega) - \sum_{ia} & \frac{K_{jb,ia}(\omega) + M_{jb,ai}(\omega)}{\epsilon_b - \epsilon_j + \omega} P_{ai}(\omega) \\ & + \sum_{ia} \frac{K_{jb,ia}(\omega) + M_{bj,ia}(\omega)}{\epsilon_b - \epsilon_j + \omega} P_{ia}(\omega) \\ & = \frac{-q}{(\epsilon_b - \epsilon_j + \omega)(\epsilon_b - \epsilon_j)} \int \psi_j(\mathbf{r}) \mathbf{j}_p \psi_b(\mathbf{r}) \mathbf{A}_0(\mathbf{r}, \omega) d\mathbf{r}, \end{aligned} \tag{3.11}$$

$$\begin{aligned} P_{bj}(\omega) - \sum_{ia} & \frac{K_{bj,ai}(\omega) + M_{bj,ia}(\omega)}{\epsilon_j - \epsilon_b + \omega} P_{ai}(\omega) \\ & + \sum_{ia} \frac{K_{bj,ai}(\omega) + M_{jb,ai}(\omega)}{\epsilon_j - \epsilon_b + \omega} P_{ia}(\omega) \\ & = \frac{-q}{(\epsilon_j - \epsilon_b + \omega)(\epsilon_j - \epsilon_b)} \int \psi_b(\mathbf{r}) \mathbf{j}_p \psi_j(\mathbf{r}) \mathbf{A}_0(\mathbf{r}, \omega) d\mathbf{r}, \end{aligned}$$

where the coupling matrix $K_{jb,ia}$ is given as

$$\begin{aligned} & K_{jb,ia}(\omega) \\ & = \frac{\omega^2 f_i}{(\epsilon_b - \epsilon_j)(\epsilon_i - \epsilon_a)} \int \psi_j(\mathbf{r}) \mathbf{j}_p \psi_b(\mathbf{r}) \mathbf{f}_{xc}(\mathbf{r}, \mathbf{r}', \omega) \psi_i(\mathbf{r}') \mathbf{j}_p \psi_a(\mathbf{r}') d\mathbf{r} d\mathbf{r}' \\ & \quad + f_i \int \psi_j(\mathbf{r}) \psi_b(\mathbf{r}) \left(\frac{1}{|\mathbf{r} - \mathbf{r}'|} + f_{xc}(\mathbf{r}, \mathbf{r}', \omega) \right) \psi_i(\mathbf{r}') \psi_a(\mathbf{r}') d\mathbf{r} d\mathbf{r}', \end{aligned} \tag{3.12}$$

and the radiative correction $M_{jb,ia}$ has the form:

$$\begin{aligned} & M_{jb,ia}(\omega) \\ & = \frac{-\omega^2 f_i}{c^2(\epsilon_j - \epsilon_b)(\epsilon_i - \epsilon_a)} \int \psi_j(\mathbf{r}) \mathbf{j}_p \psi_b(\mathbf{r}) \mathbf{G}(\mathbf{r} - \mathbf{r}') \psi_i(\mathbf{r}') \mathbf{j}_p \psi_a(\mathbf{r}') d\mathbf{r} d\mathbf{r}'. \end{aligned} \tag{3.13}$$

The above formulations (3.11) can be put in a compact form for the P-matrix elements:

$$\left[\begin{pmatrix} \mathbf{S} & \mathbf{T} \\ \mathbf{T} & \mathbf{S} \end{pmatrix} - \omega \begin{pmatrix} \mathbf{I} & \mathbf{0} \\ \mathbf{0} & \mathbf{-I} \end{pmatrix} \right] \begin{pmatrix} \mathbf{P} \\ \mathbf{P'} \end{pmatrix} = \begin{pmatrix} \mathbf{F} \\ \mathbf{-F} \end{pmatrix}, \tag{3.14}$$

with

$$\begin{aligned} & \mathbf{P}_{jb} = P_{jb}, \mathbf{P'}_{bj} = P_{bj}, \\ & \mathbf{S}_{jb,ia} = \delta_{ij}\delta_{ab}(\epsilon_i - \epsilon_a) - K_{jb,ia} - M_{jb,ia}, \\ & \mathbf{T}_{jb,ia} = K_{jb,ia} + M_{jb,ia}, \\ & \mathbf{F}_{jb} = \frac{q}{\epsilon_b - \epsilon_j} \int \psi_j(\mathbf{r}) \mathbf{j}_p \psi_b(\mathbf{r}) \mathbf{A}_0(\mathbf{r}, \omega) d\mathbf{r}. \end{aligned}$$

Furthermore, if we denote $\mathcal{P}_{jb} = P_{jb} - P_{bj}$, then from (3.14) by addition and subtraction, we can get a linear system on $\mathcal{P}_{jb}$ such that

$$(\mathcal{S} - \omega^2 \mathbf{I})\mathcal{P} = \mathcal{F}, \tag{3.15}$$

with

$$\begin{aligned} &\mathcal{S}_{jb,ia} = \delta_{ij}\delta_{ab}(\epsilon_i - \epsilon_a)^2 - 2(\epsilon_j - \epsilon_b)(K_{jb,ia} + M_{jb,ia}), \\ &\mathcal{F}_{jb} = 2(\epsilon_j - \epsilon_b)\mathbf{F}_{jb}. \end{aligned} \tag{3.16}$$

The radiative correction $M_{jb,ia}$ is a consequence of the coupling of the Maxwell equations and the linear response theory of TD-CDFT. Without the first two equations in (3.1), there will be no $M_{jb,ia}$ in (3.14), which will be reduced to the linear response within TD-CDFT [23].

3.3. Resonance condition for nano-optical structures. Besides the self-consistent determination of the induced EM field and the induced current and electron densities, the linear system (3.14) (or equivalently (3.15)) also enables us to determine the resonant eigenmodes of the nano-optical structure. Resonant eigenmodes exist for particular frequencies such that the matrix in (3.14) or (3.15) is degenerate, which can be called self-sustaining modes since they correspond to nonzero amplitudes of $\mathbf{j}$ and $\mathbf{A}$ supporting each other to form eigenmodes [6]. The resonant structure of optical spectra in general can be determined by the self-sustaining modes. Therefore, we can solve

$$\det\left(\begin{pmatrix} \mathbf{S} & \mathbf{T} \\ \mathbf{T} & \mathbf{S} \end{pmatrix} - \omega \begin{pmatrix} \mathbf{I} & \mathbf{0} \\ \mathbf{0} & \mathbf{-I} \end{pmatrix}\right) = 0, \quad \text{or} \quad \det\left(\mathcal{S} - \omega^2\mathbf{I}\right) = 0, \tag{3.17}$$

to determine the eigenfrequencies ω. In particular, we can treat it as an eigenvalue problem to determine the eigenfrequencies ω for the above matrix to have zero eigenvalues.

4. The self-consistent multiscale method. In this section, we present a multiscale scheme for the self-consistent determination of $(\delta\mathbf{A}, \delta\phi)$ and $(\delta\mathbf{j}, \delta\rho)$ described by the linearized Maxwell-KS system. We also address the issue of solving the eigenvalue problem associated with the resonant eigenfrequencies. In particular, we are interested in finding the lowest eigenvalue.

For most applications in nano-optics, the induced EM field is varying on a larger scale than the induced current and electron densities, when the wavelength of the induced EM field is comparable to or even larger than the size of the nano structure. Numerically, this difference from the scales will cause instability if the coupled Maxwell-KS equations are solved directly. As a consequence, the coupled Maxwell-KS system can be very ill-conditioned after direct space discretizations. The situation can be illustrated by the following 1-dimensional synthetic example:

$$\begin{cases} \delta\phi(x) = \displaystyle\int G(x,x')\delta\rho(x')dx', \\ \delta\rho(x) = \displaystyle\int \chi(x,x',\omega)\delta\phi(x')dx'. \end{cases} \tag{4.1}$$

We discretize (4.1) on two meshes of different scales that are appropriate for the corresponding variables. Shown in Figure 4.1 are the eigenvalues of the discretized system. It can be seen that there is a separation of scales for the eigenvalues, which is equivalent to saying that the coupled system is ill-conditioned, or stiff.

As illustrated in Figure 4.2, the Maxwell equations are solved on a much larger domain with a coarse grid compared with the smaller domain and a finer grid for TD-CDFT. In order to deal with the multiscale challenge and capture the multiple scales,

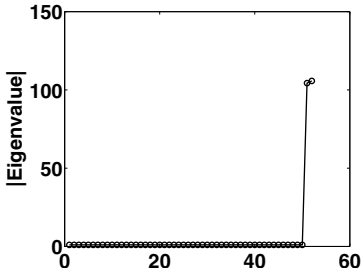

FIG. 4.1. *Eigenvalues of the discretized system of* (4.1) *when the grid size ratio of the two meshes for* (ϕ, ρ) *is set to be* $4:1$.

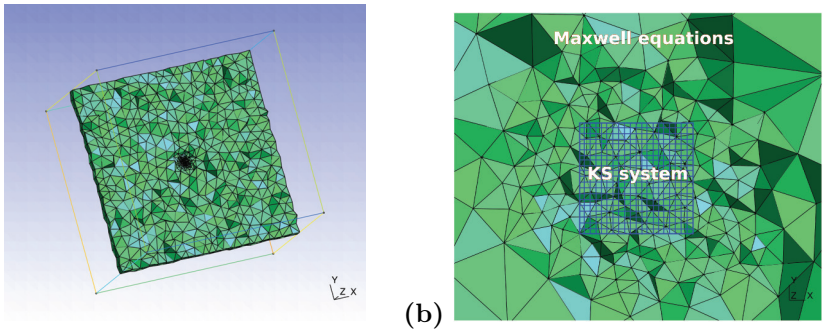

FIG. 4.2. *Domain and mesh for Maxwell equations and KS system.* (a) *Domain* $[-400,\ 400]^3$ *(a.u.) and a* 2*-dimensional slice of mesh through the nanostructure in the middle for Maxwell equations.* (b) *Zoom-in of the slice in* (a) *near the nanostructure, and domain* $[-15,\ 15]^3$ *(a.u.) and rectangular mesh for the KS system illustrated in two dimensions. In* (a)*, the triangulated mesh near the nanostructure is refined. The triangulated mesh is generated with GMSH* [12]*, consisting of* 59160 *tetrahedrons,* 73554 *edges, and* 11506 *nodes.*

we propose a multiscale scheme which consists of two solvers: TD-CDFT serving as a *micro solver* $\mathcal{T}_l$ for the current and electron densities and a *macro solver* $\mathcal{M}_d$ for the Maxwell equations. A self-consistent iteration is adopted to find the solution of the coupled system (3.1), which will lead to the following procedure:

1. *Micro solver:* at each step indexed by k, with inputs $(\delta\mathbf{A}_k, \delta\phi_k)$, update the induced current and electron densities through the linear response of TD-CDFT, i.e.,

$$(\delta\mathbf{j}_{k+1}, \delta\rho_{k+1}) = \mathcal{T}_l(\delta\mathbf{A}_k, \delta\phi_k). \tag{4.2}$$

2. *Macro solver:* with $(\delta\mathbf{j}_{k+1}, \delta\rho_{k+1})$ as fixed parameters, solve the Maxwell equations to update the induced EM field such that

$$(\delta\mathbf{A}_{k+1}, \delta\phi_{k+1}) = \mathcal{M}_d(\mathbf{j}_{k+1}, \rho_{k+1}). \tag{4.3}$$

3. Repeat until a self-consistent solution is reached.

The microsolver $\mathcal{T}_l$ can be designed to first solve the equation for the P-matrix (3.15), then obtain the induced current and electron densities through (3.8). Due to the self-consistent structure of the above algorithm, we do not have to pursue an exact solution of (3.15). Instead, a Krylov subspace method will be used to solve (3.15) approximately. For the macrosolver, we can choose a standard scheme such as the finite

difference method, finite element method, fast multipole method, etc. At each iteration, linear interpolation is used to provide the missing data due to the mismatch between the macro and micro meshes, which essentially allows communications between the macro variable of the EM field and the micro variable of the current and electron densities. The initial EM field ($\delta\mathbf{A}_0$, $\delta\phi_0$) can be chosen to be the incident light.

In a Krylov subspace method for computing the P-matrix in the micro solver, we need to evaluate the matrix $\mathcal{S}$ in the linear system (3.15), which is non-Hermitian and depends on ω nonlinearly due to the existence of the tensorial Green function and the scalar and tensor xc-kernels. The size of $\mathcal{S}$ is $occ \cdot unocc \times occ \cdot unocc$, where occ and $unocc$ are, respectively, the numbers of occupied and unoccupied KS orbitals that are solutions of the KS equation (2.11). In general the explicit form of $\mathcal{S}$ is difficult to implement for numerical computations, as a result of the complicated form of the tensor xc-kernel $\mathbf{f}_{xc}$ and the tensorial Green function $\mathbf{G}$. However, in Krylov subspace methods like the BiCGSTAB algorithm [22] used in current work, only the matrix-vector product is needed. The matrix-vector product $\mathcal{S} \cdot \mathcal{P}$ can be obtained for any vector $\mathcal{P}$ as the following:

$$\begin{aligned}[\mathcal{S} \cdot \mathcal{P}]_{jb} = (\epsilon_j - \epsilon_b)^2 \mathcal{P}_{jb} + (\epsilon_j - \epsilon_b) \int \psi_b(\mathbf{r}) \psi_j(\mathbf{r}) \delta v_{KS}(\mathbf{r}) d\mathbf{r} \\ + 2\omega \left(\int \psi_b(\mathbf{r}) \mathbf{j}_p \psi_j(\mathbf{r}) \delta\mathbf{A}(\mathbf{r}) d\mathbf{r} + \int \psi_b(\mathbf{r}) \mathbf{j}_p \psi_j(\mathbf{r}) \delta\mathbf{A}_{xc}(\mathbf{r}) d\mathbf{r} \right).\end{aligned} \tag{4.4}$$

Therefore at the kth step in the micro solver, the right-hand side of the above equality can be computed using $\delta\mathbf{A}_k$, the current density $\delta\mathbf{j}_k$, and the electron density $\delta\rho_k$ through (3.2)–(3.3), which will give the matrix $\mathcal{S}_k$ needed. Then one step of the Krylov subspace solver applied on $\mathcal{P}_k$ from the previous step will give an approximate solution of (3.15) such that

$$(\mathcal{S}_k - \omega^2)\mathcal{P}_{k+1} \approx \mathcal{F}. \tag{4.5}$$

Then $\mathcal{P}_{k+1}$ can be used to update $\delta\mathbf{j}_{k+1}$ and $\delta\rho_{k+1}$.

As explained previously, the resonant eigenmodes or eigenfrequencies of the nano-optical response correspond to the frequencies ω such that $\mathcal{S} - \omega^2\mathbf{I}$ has a zero eigenvalue. In particular, we are interested in computing the lowest eigenvalue. We use an iterative Jacobi–Davidson scheme [1] to solve this eigenvalue problem. Since $\mathcal{S}$ depends on ω, we start with an initial guess of ω, say ω_0, update $\mathcal{S}$ during the iterations, say $\mathcal{S}_l$ at iteration l, with one iteration of the multiscale scheme for each updated value of ω, say ω_l, until a certain convergence criterion is satisfied.

For applications considered in current work, we assume the systems to be in a vacuum. At the microscopic level, we choose a large enough cubic domain containing the molecular structures under consideration. We use the package OCTOPUS [5], which adopts real-space finite difference methods on structured meshes, to obtain the ground state KS orbitals by solving the ground state KS equations (2.11). The setup is illustrated in Table 5.1 in section 5. Periodic boundary conditions are imposed in OCTOPUS for our applications. For the macroscopic variables, the Maxwell equations are solved with a hybrid nodal-edge finite element method on a triangulated mesh (e.g., see [15]). For our applications, the impedance boundary condition is imposed [15],

$$\mathbf{n} \times (\nabla \times \boldsymbol{E}) - iq\mathbf{n} \times (\mathbf{n} \times \boldsymbol{E}) = 0,$$

where $\mathbf{n}$ is the outward normal to the boundary. Alternative implementations of the scheme will be for future investigations.

TABLE 5.1
Self-sustaining eigenmode of molecules.

Self-sustaining eigenmodes: Lowest eigenvalue				
Sample	CH_4	SiH_4	C_2H_6	$C_{12}H_{10}N_2$
Eigenfrequency ω (a.u.)	0.3452[a]	0.3053[b]	0.3165[c]	0.1398
occ	4	4	7	34
unocc	8	8	14	34
Domain of time-dependent KS (a.u.)	$[-10,\ 10]^3$	$[-10,\ 10]^3$	$[-15,\ 15]^3$	$[-15,\ 15]^3$
Mesh of time-dependent KS	$21 \times 21 \times 21$	$21 \times 21 \times 21$	$31 \times 31 \times 31$	$31 \times 31 \times 31$
Mesh size for time-dependent KS (a.u.)	1.0	1.0	1.0	1.0
Domain of Maxwell (a.u.)	$[-400,\ 400]^3$	$[-400,\ 400]^3$	$[-400,\ 400]^3$	$[-400,\ 400]^3$
Number of iterations in Jacobi–Davidson	11	11	17	156
Setup in OCTOPUS for solving ground state KS (2.11)				
Domain (a.u.)	$[-10,\ 10]^3$	$[-10,\ 10]^3$	$[-15,\ 15]^3$	$[-15,\ 15]^3$
Mesh	$41 \times 41 \times 41$	$41 \times 41 \times 41$	$61 \times 61 \times 61$	$61 \times 61 \times 61$
Mesh size (a.u.)	0.5	0.5	0.5	0.5

[a] 0.34540 (a.u.), Ref. NIST Chemistry WebBook. http://cccbdb.nist.gov/gap3.asp?method=61&basis=10
[b] 0.30306 (a.u.), Ref. NIST Chemistry WebBook. http://cccbdb.nist.gov/gap3.asp?method=61&basis=10
[c] 0.32845 (a.u.), Ref. NIST Chemistry WebBook. http://cccbdb.nist.gov/gap3.asp?method=61&basis=21

5. Numerical examples. We apply the linear response formulations to study the optical response of several molecules: methane (CH_4), silane (SiH_4), ethane (C_2H_6), and *trans*-azobenzene ($C_{12}H_{10}N_2$). Assume the molecule is centered at $(0, 0, 0)$ in the *x-y-z* coordinate representation. We first calculate the self-sustaining eigenmodes for these structures, especially the lowest eigenvalue. The results are listed in Table 5.1. The tolerance as the convergence criterion is chosen to be 10^{-8} in the Jacobi–Davidson scheme. The correction equation in the Jacobi–Davidson scheme is solved with the BiCGSTAB algorithm with relative residual reduction equal to 10^{-5}. We choose a Jacobi-like preconditioner which uses the diagonal terms $[\delta_{ij}\delta_{ab}(\epsilon_i - \epsilon_a)^2 - \omega^2]_{ia,jb}$ as a preconditioner. When solving the Maxwell equations with the hybrid nodal-edge finite element method (e.g., see [15] and Figure 4.2), a D-LU-preconditioned QMR algorithm [11, 2] is applied to solve the resulting discretized system with the relative residual reduction chosen to be 10^{-8}. The triangulated mesh is generated by GMSH [12] and consists of 59160 tetrahedrons, 73554 edges, and 11506 nodes. As shown in Figure 4.2, the mesh is refined near the nanostructure to capture the small scale.

Next, we verify our computation by studying the response spectra. The incident field is chosen to be

$$\mathbf{A}_0(\mathbf{r}, \omega) = \mathbf{p} c e^{i\frac{\omega}{c}\mathbf{d}\cdot\mathbf{r}}/i\omega,$$

with $\mathbf{p} = (p_x, p_y, p_z)$, $\mathbf{d} = (d_x, d_y, d_z)$ such that $||\mathbf{p}|| = 1$, $||\mathbf{d}|| = 1$, and $\mathbf{p} \cdot \mathbf{d} = 0$. When a molecule is placed in an electric field it acquires an induced dipole moment given as

$$\delta\mu(\omega) = -\int \mathbf{r}\delta\rho(\mathbf{r}, \omega)d\mathbf{r}. \tag{5.1}$$

Using the continuity equation (3.7), we can rewrite the induced dipole moment in terms of the induced current density,

$$\delta\mu(\omega) = \frac{i}{\omega}\int \delta\mathbf{j}(\mathbf{r}, \omega)d\mathbf{r}. \tag{5.2}$$

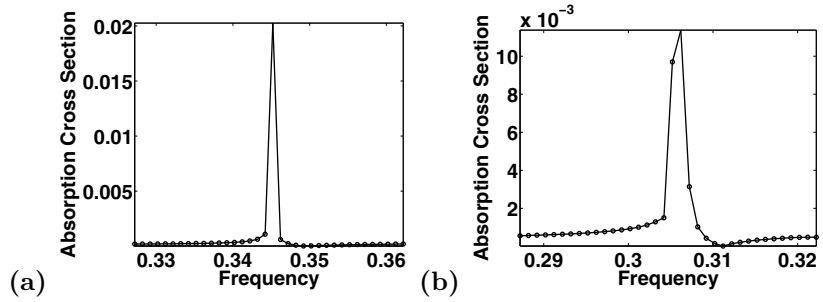

FIG. 5.1. *Absorption cross section* $|\sigma|$*:* (a) CH_4*, and* (b) SiH_4*. Units for frequencies: a.u.*

TABLE 5.2
Self-sustaining eigenmode of CH_4*: lowest eigenvalue. Units: a.u. The Maxwell equations are solved numerically with different choices of relative residual reduction.*

Relative residual reduction for solving Maxwell equations	Eigenfrequency	# iteration of Jacobi–Davidson scheme	CPU time (seconds)
10^{-8}	0.345235516198412	11	8.663e3
$\max\{10^{-8}, 10^{-2}/2^{n-1}\}$	0.345235516228593	11	7.069e3
10^{-5}	0.345235516195180	11	5.805e3
$\max\{10^{-5}, 10^{-2}/2^{n-1}\}$	0.345235516227064	11	5.557e3

With this incident field and given frequencies, we solve (3.15) to get the induced current density and the induced EM field.

The induced dipole moment and the EM field are related through the linear polarizability $\vec{\alpha}$ as

$$\delta\mu = \vec{\alpha}\delta\mathbf{E};\ \vec{\alpha} = \begin{pmatrix} \alpha_{xx} & \alpha_{xy} & \alpha_{xz} \\ \alpha_{yx} & \alpha_{yy} & \alpha_{yz} \\ \alpha_{zx} & \alpha_{zy} & \alpha_{zz} \end{pmatrix}. \tag{5.3}$$

Hence we can compute $\vec{\alpha} = \frac{\delta\mu}{\delta\mathbf{E}}$. In particular, we compute the absorption cross section

$$\sigma(\omega) = \frac{4\pi\omega\Im\alpha_{av}}{c},$$

with $\alpha_{av} \equiv \frac{\alpha_{xx}+\alpha_{yy}+\alpha_{zz}}{3}$. That is, σ is proportional to the imaginary part of α_{av}. Figure 5.1 shows the results of σ for CH_4 and SiH_4. The results confirm that the computed lowest eigenvalue in Table 5.1 is a resonant mode because in Figure 5.1(a) we observe a peek at $\omega \approx 0.3452$ (a.u.), and in Figure 5.1(b) we observe a peek at $\omega \approx 0.3053$ (a.u.).

In the macro solver for the EM field, we can choose to solve the Maxwell equations with a larger relative residual reduction compared with the micro solver for the microscopic quantities. In practice, we can choose the relative residual reduction for solving the Maxwell equations dynamically. Table 5.2 shows the results for computing the lowest eigenfrequency of CH_4 by choosing the relative residual reduction according to $\max\{10^{-8}, 10^{-2}/2^{n-1}\}$, where n is the nth iteration of solving the correction equation in the Jacobi–Davidson algorithm. Furthermore, we test our multiscale solver by choosing even larger relative residual reduction 10^{-5} and $\max\{10^{-5}, 10^{-2}/2^{n-1}\}$.

6. Conclusion. In order to reduce the complexity for solving the many-body Schrödinger equation, we incorporate the time-dependent current density functional

theory into the semiclassical theory for studying nano-optical responses. The system is described by the coupled Maxwell-KS equations that determine the induced EM field and the induced current and electron densities self-consistently. A linear system is formulated within the linear response theory. The eigenmodes of the nano-optical response exist at frequencies such that the linear system is degenerate or has a zero eigenvalue. A multiscale method is designed to solve the ill-conditioned linear system. Response spectra of sample molecules, such as methane, silane, ethane, and *trans*-azobenzene, are studied and resonance eigenmodes are observed.

Appendix A. *P*-matrix. In this appendix, we justify the spectral representation (3.8) and (3.10) by showing that they are consistent with the last two equations in (3.1). Let us focus on (3.8) here. The argument for (3.10) will be similar. By substituting the linear response function $\chi_{\alpha\beta}$ into the induced electron density $\delta\rho$ in the 4th equation of (3.1), we have

$$\begin{aligned}\delta\rho(\mathbf{r},\omega) = &\int \sum_{ia} f_i \left[\left(\frac{\psi_i(\mathbf{r})\psi_a(\mathbf{r})\psi_a(\mathbf{r}')\mathbf{j}_p\psi_i(\mathbf{r}')}{\epsilon_i-\epsilon_a+\omega} \right) - \left(\frac{\psi_i(\mathbf{r})\psi_a(\mathbf{r})\psi_a(\mathbf{r}')\mathbf{j}_p\psi_i(\mathbf{r}')}{\epsilon_a-\epsilon_i+\omega} \right)^* \right] \\ &\cdot \delta\mathbf{A}_{KS}(\mathbf{r}',\omega)d\mathbf{r}' \\ &+ \int \sum_{ia} f_i \left[\left(\frac{\psi_i(\mathbf{r})\psi_a(\mathbf{r})\psi_a(\mathbf{r}')\psi_i(\mathbf{r}')}{\epsilon_i-\epsilon_a+\omega} \right) - \left(\frac{\psi_i(\mathbf{r})\psi_a(\mathbf{r})\psi_a(\mathbf{r}')\psi_i(\mathbf{r}')}{\epsilon_a-\epsilon_i+\omega} \right)^* \right] \\ &\cdot \delta v_{KS}(\mathbf{r}',\omega)d\mathbf{r}',\end{aligned}$$

which can be simplified as

$$\begin{aligned}\delta\rho(\mathbf{r},\omega) = &\sum_{ia} f_i\psi_i(\mathbf{r})\psi_a(\mathbf{r}) \left(\frac{1}{\epsilon_i-\epsilon_a+\omega} \right) \\ &\times \left[\frac{-\omega}{\epsilon_i-\epsilon_a} \int \psi_a(\mathbf{r}')\mathbf{j}_p\psi_i(\mathbf{r}')\cdot\delta\mathbf{A}_{KS}(\mathbf{r}',\omega)d\mathbf{r}' + \int \psi_a(\mathbf{r}')\psi_i(\mathbf{r}')\delta v_{KS}(\mathbf{r},\omega)d\mathbf{r} \right] \\ &- f_i\psi_i(\mathbf{r})\psi_a(\mathbf{r}) \left(\frac{1}{\epsilon_a-\epsilon_i+\omega} \right) \\ &\times \left[\frac{-\omega}{\epsilon_a-\epsilon_i} \int \psi_i(\mathbf{r}')\mathbf{j}_p\psi_a(\mathbf{r}')\cdot\delta\mathbf{A}_{KS}(\mathbf{r},\omega) + \int \psi_a(\mathbf{r}')\psi_i(\mathbf{r}')\delta v_{KS}(\mathbf{r}',\omega)d\mathbf{r} \right],\end{aligned}$$

which, by definition of P-matrix, is equivalent to

$$\delta\rho(\mathbf{r},\omega) = \sum_{ia} f_i\psi_i(\mathbf{r})\psi_a(\mathbf{r})P_{ai} - f_i\psi_a(\mathbf{r})\psi_i(\mathbf{r})P_{ia} = \sum_{ia} f_i\psi_i(\mathbf{r})\psi_a(\mathbf{r})[P_{ai}-P_{ia}].$$

Acknowledgments. The authors would like to thank the anonymous referees for helpful suggestions on this work. They are also grateful to Dr. Chao Yang and Dr. Guanghui Hu for fruitful discussions on this work.

REFERENCES

[1] Z. Bai, J. Demmel, J. Dongarra, A. Ruhe, and H. van der Vorst, eds., *Templates for the Solution of Algebraic Eigenvalue Problems: A Practical Guide*, SIAM, Philadelphia, 2000.

[2] R. Barrett, M. W. Berry, T. F. Chan, J. Demmel, J. Donato, J. Dongarra, V. Eijkhout, R. Pozo, C. Romine, and H. van der Vorst, *Templates for the Solution of Linear Systems: Building Blocks for Iterative Methods*, SIAM, Philadelphia, 1994.

[3] G. F. Bertsch, J.-I. Iwata, A. Rubio, and K. Yabana, *Real-space, real-time method for the dielectric function*, Phys. Rev. B, 62 (2000), pp. 7998–8002.
[4] M. E. Casida, *Time-dependent density functional response theory for molecules*, in Recent Advances in Density Functional Methods, D. P. Chong, ed., World Scientific, Singapore, 1995, pp. 155–193.
[5] A. Castro, H. Appel, M. Oliveira, C. A. Rozzi, X. Andrade, F. Lorenzen, and M. A. L. Marques, *Octopus: A tool for the application of time-dependent density functional theory*, Phys. Stat. Sol. B, 243 (2006), pp. 2465–2488.
[6] K. Cho, *Optical Response of Nanostructures: Microscopic Nonlocal Theory*, Springer, New York, 2003.
[7] C. Cohen-Tannoudji, J. Dupont-Roc, and G. Grynberg, *Photons and Atoms: Introduction to Quantum Electrodynamics*, Wiley, New York, 1989.
[8] P. A. M. Dirac, *Note on exchange phenomena in the Thomas atom*, Proc. Cambridge Phil. Soc., 26 (1930), pp. 376–385.
[9] W. E, J. Lu, and X. Yang, *Effective Maxwell equations from time-dependent density functional theory*, Acta Math. Sinica, 27 (2011), pp. 339–368.
[10] C. Fiolhais, F. Nogueira, and M. A. L. Marques, eds., *A Primer in Density Functional Theory*, Lecture Notes in Phys. 620, Springer, New York, 2003.
[11] R. Freund and N. Nachtigal, *QMR: A quasi-minimal residual method for non-Hermitian linear systems*, Numer. Math., 10 (1991), pp. 315–339.
[12] C. Geuzaine and J.-F. Remacle, *GMSH: A three-dimensional finite element mesh generator with built-in pre- and post-processing facilities*, Internat. J. Numer. Methods Engrg., 79 (2009), pp. 1309–1331.
[13] S. K. Ghosh and A. K. Dhara, *Density-functional theory of many-electron systems subjected to time-dependent electric and magnetic fields*, Phys. Rev. A, 38 (1988), pp. 1149–1158.
[14] P. Hohenberg and W. Kohn, *Inhomogeneous electron gas*, Phys. Rev., 136 (1964), pp. 864–871.
[15] J. M. Jin, *The Finite Element Method in Electromagnetics*, 2nd ed., Wiley, New York, 2002.
[16] O. Keller, *Local fields in the electrodynamics of mesoscopic media*, Phys. Rep., 268 (1996), pp. 85–262.
[17] W. Kohn and L. J. Sham, *Self-consistent equations including exchange and correlation effects*, Phys. Rev., 140 (1965), pp. 1133–1138.
[18] N. T. Maitra, I. Souza, and K. Burke, *Current-density functional theory of the response of solids*, Phys. Rev. B, 68 (2003), 045109.
[19] M. A. L. Marques, C. A. Ullrich, F. Nogueira, A. Rubio, K. Burke, and E. K. U. Gross, eds., *Time-Dependent Density Functional Theory*, Lecture Notes in Phys. 706, Springer, Heidelberg, 2006.
[20] E. Runge and E. K. U. Gross, *Density-functional theory for time-dependent systems*, Phys. Rev. Lett., 52 (1984), pp. 997–1000.
[21] A. Stahl and I. Balslev, *Electrodynamics of the Semiconductor Band Edge*, Springer Tract Modern Phys. 110, Springer, New York, 1987.
[22] H. A. van Der Vorst, *Bi-CGSTAB: A fast and smoothly converging variant of Bi-CG for the solution of nonsymmetric linear systems*, SIAM J. Sci. Statist. Comput., 13 (1992), pp. 631–644.
[23] M. van Faassen, P. L. de Boeij, R. van Leeuwen, J. A. Berger, and J. G. Snijders, *Application of time-dependent current-density-functional theory to nonlocal exchange-correlation effects in polymers*, J. Chem. Phys., 118 (2003), pp. 1044–1053.
[24] G. Vignale, *Current-dependent exchange-correlation potential for dynamical linear response theory*, Phys. Rev. Lett., 77 (1996), pp. 2037–2040.
[25] G. Vignale, C. A. Ullrich, and S. Conti, *Time-dependent density functional theory beyond the adiabatic local density approximation*, Phys. Rev. Lett., 79 (1997), pp. 4878–4881.
[26] S. H. Vosko, L. Wilk, and M. Nusair, *Accurate spin-dependent electron liquid correlation energies for local spin density calculations: A critical analysis*, Canad. J. Phys., 58 (1980), pp. 1200–1211.